Electronic Supplementary Material (ESI) for Lab on a Chip.

Supporting Information

Sustained delivery of focal ischemia coupled to real-time neurochemical sensing in brain slices

Michael T. Cryan[1], Yuxin Li[1], and Ashley E. Ross[1,2]

[1]University of Cincinnati
Department of Chemistry
312 College Drive
404 Crosley Tower
Cincinnati, OH 45221-0172

Office #: 513-556-9314
Email: Ashley.ross@uc.edu

[2]Corresponding author

SUPPLEMENTAL MOVIES

Supplemental Movie 1: Delivery of fluorescein in a slice of 4% agarose over 60 s with the straddling channels turned off and the stimulus flow at 1 μL/min. This experiment served as a control within agarose. Removing flow from the straddling channels resulted in decreased spatial resolution over time (see Fig. 2D), providing evidence that the straddling channels contribute to the localization of the stimulus. This is a time lapse video (3× speed) of the micrographs shown in Fig. S2C-D.

Supplemental Movie 2: Delivery of fluorescein in a slice of rat caudate putamen over 60 s with a stimulus-to-containment flow ratio of 1:10. The stimulus remains contained within the region of interest when the straddling channels are turned on. In agarose, average spread after 60 s using the 1:10 ratio was more stable than delivery using the 1:1 (see Fig. S3A); in tissue, the 1:1 had improved stability compared to the same ratio used in agarose, likely due to the tissue matrix restricting lateral diffusion (see Fig. 4A). This is a time lapse video (3× speed) of the micrographs shown in Fig. 3A-D.

Supplemental Movie 3: Delivery of fluorescein in a slice of rat caudate putamen for 60 s with the straddling channels turned off and the stimulus flow at 1 μL/min. This experiment served as a control within the tissue matrix. Similar to delivery in agarose (see Supplementary Movie 1), removing flow from the straddling channels resulted in decreased and non-sustained spatial resolution over time, providing evidence that the straddling channels contribute to the localization of the stimulus within the brain tissue matrix. This is a time lapse video (3× speed) of the micrographs shown in Fig. 3F-I.

SUPPLEMENTAL METHODS

Reagents

All chemicals were purchased from Fisher Scientific (Fair Lawn, NJ, USA) unless otherwise noted. Aqueous solutions were made with Milli-Q deionized water (Millipore, Billerica, MA, USA). The agarose experiments used Tris buffer consisting of 15 mM Tris(hydroxymethyl)aminomethane, 1.25 mM NaH_2PO_4, 2.0 mM Na_2SO_4, 3.25 mM KCl, 140 mM NaCl, 1.2 mM $CaCl_2$ dihydrate, and 1.2 mM $MgCl_2$ hexahydrate that was maintained at a physiological pH of 7.4. *Ex vivo* tissue experiments used artificial cerebrospinal fluid (aCSF) solutions consisting of 2.5 mM KCl, 1.2 mM NaH_2PO_4, 2.4 mM $CaCl_2$ dihydrate, 1.2 mM $MgCl_2$ hexahydrate, 126 mM NaCl, 11 mM *D*-glucose, 25 mM sodium bicarbonate, and 15 mM Tris(hydroxymethyl)aminomethane. The ischemic aCSF used in the dopamine experiments was similar to regular aCSF but was deoxygenated with nitrogen and had *D*-glucose removed to simulate ischemia. Solutions of fluorescein were used for quantitating spread of stimulus in tissue (1.0 mg/mL in aCSF) and in agarose (0.1 mg/mL in Tris buffer). Aliquots of Image-iT Green Hypoxia Reagent (Thermo Fisher Scientific, Waltham, MA, USA) were dissolved in aCSF to compare local vs. global hypoxia in tissue.

Electrode fabrication

To make carbon-fiber microelectrodes, 7-µm T-650 carbon fibers (Mitsubishi Chemical Carbon Fiber and Composites, Sacramento, CA, USA) were aspirated into 1.2 × 0.68 mm glass capillaries (A&M Systems, Sequim, WA, USA) and pulled into two using a vertical Narishige PE-22 Electrode Puller (Tokyo, Japan). Fibers were manually cut 150-200 µm from the glass seal using a scalpel under a microscope. Electrodes were bathed in isopropyl alcohol for a minimum of 10 minutes prior to use and were backfilled with 1 M KCl supporting electrolyte.

COMSOL Multiphysics modeling

A Cartesian computational model was used to predict the lateral spread of the stimulus as it exited the microchannel and spread within a complex matrix. This model predicts spread as a function of initial stimulus concentration, the flow rates through the stimulus and straddling channels, and time. We rendered the simulation with COMSOL Multiphysics 5.4 (COMSOL Multiphysics, Burlington, MA, USA) to study the spread of stimulus as it was delivered to agarose. The model used the incompressible flow and Navier-Stocks equation of mass transfer to describe the spread and convection within the porous media (COMSOL modules: Free and Porous Media Flow; Transport of Diluted Species in Porous Media). Figs. 2, S4, and S6 depict top view simulated COMSOL images, similar to images collected experimentally. We modeled fluid flow through the 200-μm-wide straddling channels and a single 100-μm-wide stimulus channel. The fluorescein solution was modeled using a reported diffusion coefficient (4.25×10^{-6} cm^2 s^{-1});[36] the velocity through the stimulus port was set to 3.3×10^{-3} m/s (flow rate is 1 μL/min through a 100-μm-wide port) and 1.7×10^{-2} m/s through the straddling ports (flow rate is 10 μL/min through 200-μm-wide ports). As a simulated control, the straddling ports were completely deleted (Fig. 2B and Fig. S4B) to provide evidence that straddling channels are necessary for containing the localized spread in the matrix over time. The matrix that the flow was delivered to was modeled as a porous 400-μm-thick matrix of 4% agarose as previously described.[37] In this simulation, the agarose gel's porosity was 0.9805 and the Darcy permeability of agarose was 249 nm^2.[37–39] The initial concentration in the two straddling channels was set to zero, and the center stimulus channel was set to 0.5 mg/mL. This is depicted as "intensity" in Figs. 2, S4, and S6. The model was solved using a triangular mesh. We used time-dependency to solve for mass transport. The delivery time and inflow flow rate through the straddling channels were varied at 1 and 10 μL/min to test the effect of flow localization, with the stimulus flow set at 1 μL/min. We also ran the model without the straddling channels present to demonstrate their effectiveness at containing the spread of the stimulus (Fig. 2B and Fig. S4B). In addition, delivery was simulated for 30 minutes with the

containment flow on and off (Fig. S4). The delivery of a “hypoxic” stimulus was also simulated over 30 minutes (Fig. S6) and compared to the fluorescein stimulus; the hypoxic stimulus was simulated by monitoring the spread of N_2 gas in the porous matrix. This is because in ischemic buffer, oxygen is removed and replaced with N_2. The diffusion coefficient of N_2 in water (2×10^{-5} cm^2 s^{-1}) was used in this model.

Statistics: All values are reported as mean ± standard error of the mean (SEM) unless otherwise noted. All statistics and curve fitting were performed in GraphPad Prism 8 (GraphPad Software, Inc., La Jolla, CA, USA). Values were considered significant at the 95 % confidence interval ($p < 0.05$). All n values represent either number of agarose or tissue slices, unless otherwise stated in the text.

SUPPLEMENTAL FIGURES

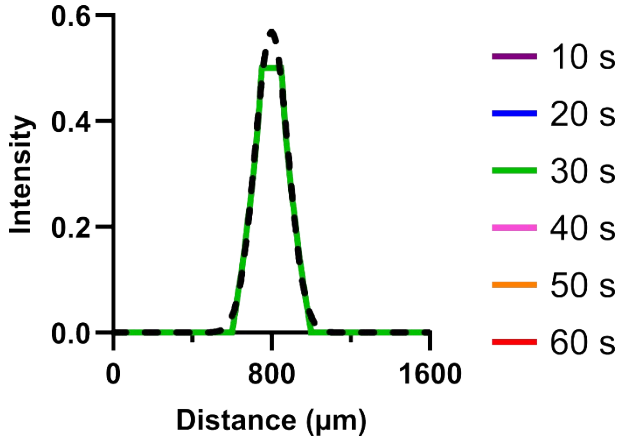

Figure S1: Prediction of Gaussian distribution in COMSOL for 60 s of stimulus delivery with the straddling channels turned on. All time points are plotted and superimposed on the graph and show extremely nominal change in spatial resolution over 60 s. The 60 s curve was fit with Gaussian distribution (dotted black trace, $r^2 = 0.99$).

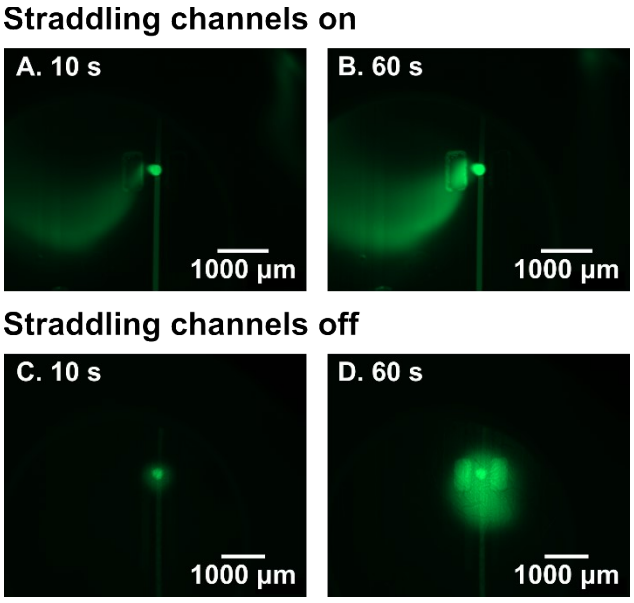

Figure S2: Spreading of fluorescein within slices of 4% agarose was observed over 60 s with the straddling channels on (A and B) and off (C and D). Stimulus flow was 1 µL/min in all images and straddling channel flow was 10 µL/min when turned on. The stimulus is contained within the slice when flow from the straddling channels is turned on (A and B). The plume of fluorescence seen in both images (A and B) is fluorescein suspended in solution after successfully exiting through the top of the agarose slice since when the straddling channels are turned on, it forces the stimulation solution out of the top of the slice. When the straddling channel flow is off, the stimulus spreads without containment and radial diffusion is observed within the agarose slice (C and D). We also do not observe obvious fluorescein exiting out of the top of the agarose slice because the stimulus is able to spread radially unencumbered. This validates the efficacy of the containment channels in focusing the stimulus.

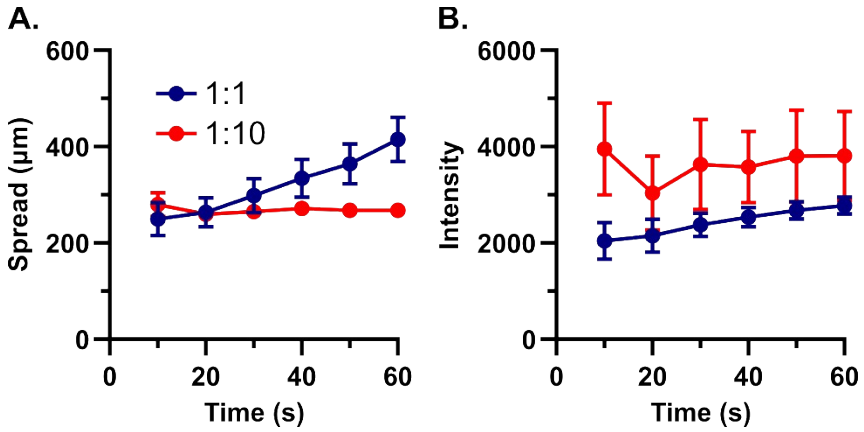

Figure S3: A 1:10 stimulus-to-containment flow rate offers enhanced spatial resolution in slices of 4% agarose (n = 9). (A) Stimulus spread was observed over 60 s at the 1:1 and 1:10 flow ratios. More resolved delivery was seen at the 1:10 ratio, with a maximum spread of 267.9 ± 12 µm after 60 s, compared to 415.0 ± 46 µm using the 1:1. Using the 1:10 ratio results in more stable stimulus delivery as compared to using the 1:1, which trends upwards over time. Improved spatial resolution in agarose using the 1:10 ratio agrees with similar experiments conducted in tissue. (B) Fluorescence intensity was recorded over the same time period for both flow ratios. There was a significant difference between the 1:1 and the 1:10 flow ratios after 60 s of delivery (paired t-test, p = 0.0128).

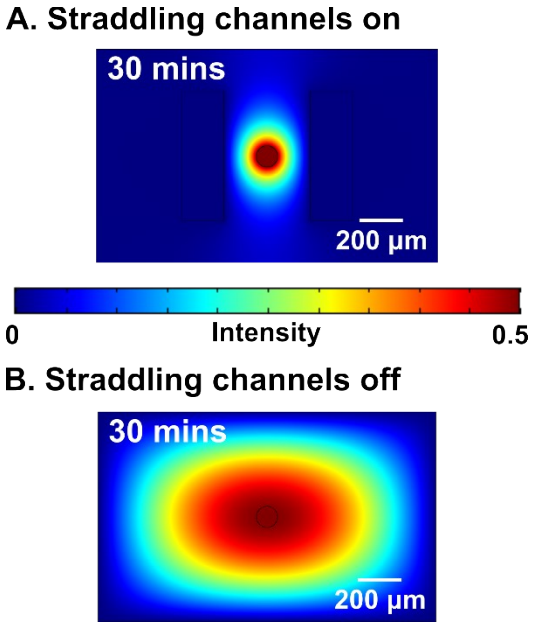

Figure S4: Containment of stimulus is still achieved after 30 mins of stimulus delivery with flow coming out of the straddling channels. This is a continuation of the simulated data shown in Fig. 2. The stimulus is shown in false color. (A) Simulated stimulus spread in a porous matrix after 30 minutes of delivery with the straddling channels on. The stimulus, flowing at 1 µL/min, is still contained by flow out of the straddling channels at 10 µL/min. (B) Stimulus spatial resolution is attenuated following 30 mins of unrestricted flow. In this simulation, the containment channels have been deleted from the model. Without containment flow, the stimulus (flowing at 1 µL/min) spreads largely unencumbered within the simulated porous matrix.

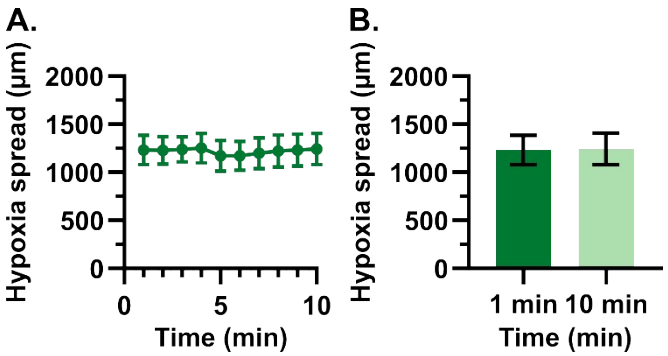

Figure S5: Delivery of local hypoxia is stable over a 10-min period (*n* = 8). A 1:1 flow ratio was used to deliver stimulation to tissue. Total hypoxia spread was 1232 ± 152.4 µm after 1 min and 1243 ± 164.2 µm after 10 mins. There was no significant difference in spread following 10 mins of hypoxia administration (paired *t*-test, ns).

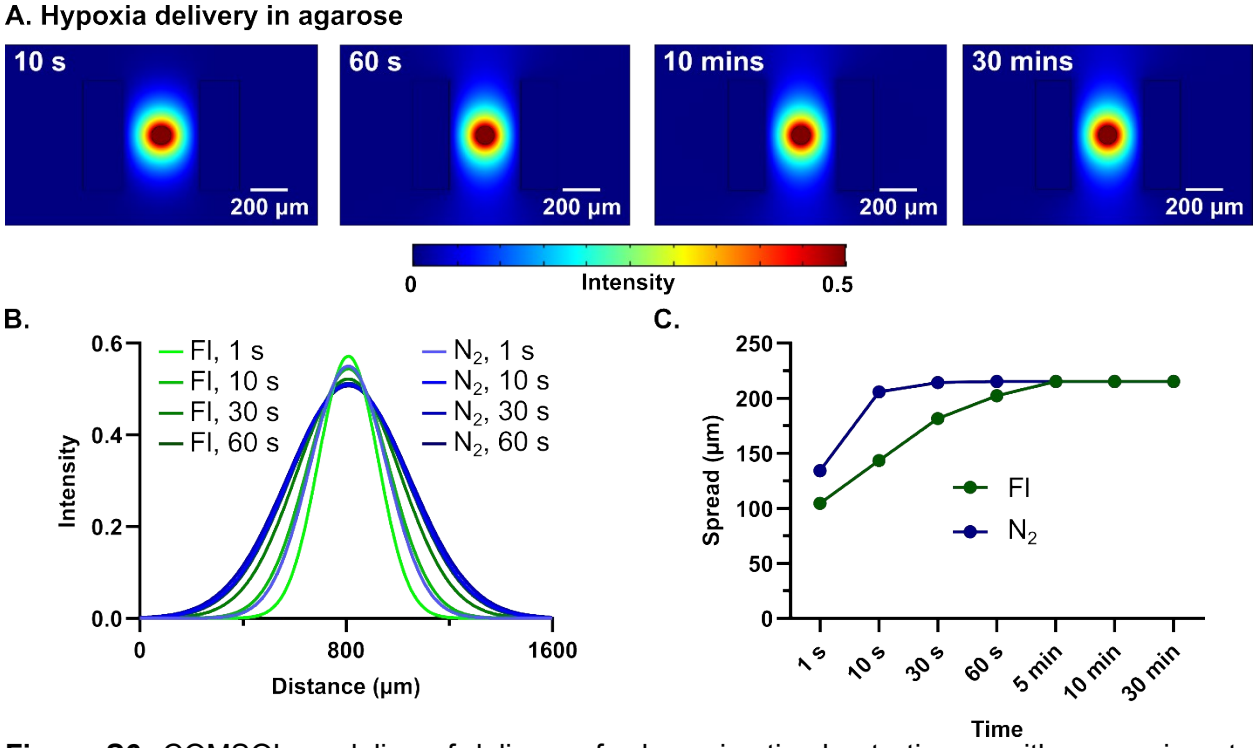

Figure S6: COMSOL modeling of delivery of a hypoxic stimulus to tissue, with comparison to fluorescein stimulation. (A) Delivery of a hypoxic stimulus to agarose from 10 s to 30 mins. The "hypoxic" stimulus was characterized by the diffusion coefficient of N_2; we used N_2 here since we bubble in N_2 gas for deoxygenation of the stimulus during the experiment. The stimulus is shown in false color. From 10 s to 30 mins of delivery, the stimulus remains localized when the adjacent containment channels are turned on. (B) Simulated distance vs. intensity plots for both fluorescein (Fl, green) and nitrogen (N_2, blue) delivery from 1 s to 60 s. From these plots, we observe that the N_2 stimulus spreads out in a shorter amount of time then the Fl stimulus; we attribute this disparity to differences in the diffusion coefficients of each analyte. Although N_2 spreads out faster, by 60 s the plots of both analytes are proximal in resolution due to containment of the stimulus by the straddling channels. (C) Simulated time vs. spread plot for both analytes. As seen in panel B, the N_2 stimulus reaches its maximum spread in a shorter amount of time than Fl; however, after 60 s, the spread of each analyte substantially overlaps given containment from the straddling channels. The different analyte diffusion coefficients demonstrate their effect on spread only within the first 60 s of delivery, before both N_2 and Fl reach a terminal spread lasting up to 30 mins.

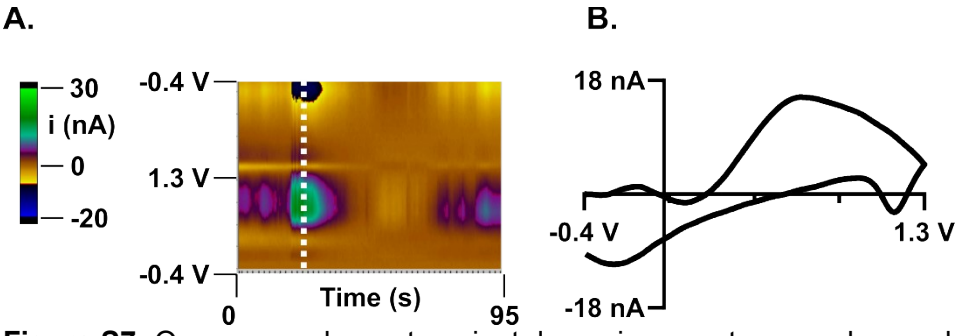

Figure S7: On average, larger transient dopamine events were observed during local ischemia. (A) Example false color plot, line indicates where representative CV in (B) was taken.

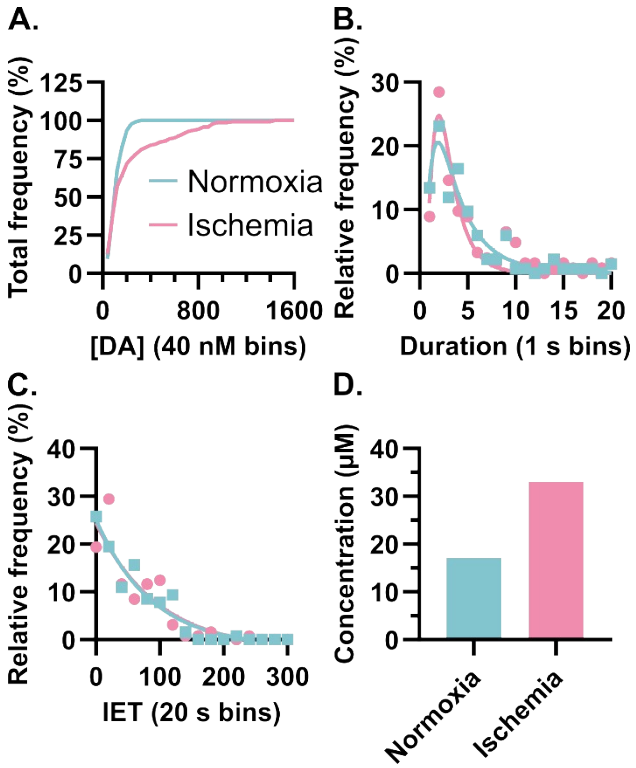

Figure S8: An increase in total dopamine concentration is observed during application of local ischemia to tissue (*n* = 9). (A) A wider distribution of dopamine concentrations occurs during ischemia compared to control normoxic conditions. This is due to larger transients occurring during the injury period. (B) There is a wider distribution of dopamine event durations during normoxia as compared to ischemia. Although there is a wider distribution of normoxic events, the average duration is much larger during local ischemia (Fig. 7B). (C) The distribution of interevent times is similar between normoxia and ischemia, creating considerable distribution curve overlap. (D) Total dopamine concentration is elevated during ischemia when compared to normoxia and controlled for time. Cumulative dopamine concentration was 17.1 µM during normoxia and 33.0 µM during ischemia, representing a 1.93-fold increase in dopamine content during injury.